HHS Public Access

Author manuscript

Biomaterials. Author manuscript; available in PMC 2017 January 01.

Published in final edited form as:

Biomaterials. 2016 January ; 77: 186–197. doi:10.1016/j.biomaterials.2015.11.018.

Poly(ethylene glycol) hydrogels with cell cleavable groups for autonomous cell delivery

Mrityunjoy Kar[a], **Yu-Ru Vernon Shih**[a], **Daniel Ortiz Velez**[a], **Pedro Cabrales**[a], and **Shyni Varghese**[a,*]

[a]Department of Bioengineering, University of California, San Diego, La Jolla, California, USA

Abstract

Cell-responsive hydrogels hold tremendous potential as cell delivery devices in regenerative medicine. In this study, we developed a hydrogel-based cell delivery vehicle, in which the encapsulated cell cargo control its own release from the vehicle in a protease-independent manner. Specifically, we have synthesized a modified poly(ethylene glycol) (PEG) hydrogel that undergoes degradation responding to cell-secreted molecules by incorporating disulfide moieties onto the backbone of the hydrogel precursor. Our results show the disulfide-modified PEG hydrogels disintegrate seamlessly into solution in presence of cells without any external stimuli. The rate of hydrogel degradation, which ranges from hours to months, is found to be dependent upon the type of encapsulated cells, cell number, and fraction of disulfide moieties present in the hydrogel backbone. The differentiation potential of human mesenchymal stem cells released from the hydrogels is maintained *in vitro*. The *in vivo* analysis of these cell-laden hydrogels, through a dorsal window chamber and intramuscular implantation, demonstrated autonomous release of cells to the host environment. The hydrogel-mediated implantation of cells resulted in higher cell retention within the host tissue when compared to that without a biomaterial support. Biomaterials that function as a shield to protect cell cargos and assist their delivery in response to signals from the encapsulated cells could have a wide utility in cell transplantation and could improve the therapeutic outcomes of cell-based therapies.

Keywords

Hydrogel; cell-responsive biomaterial degradation; stem cells; cell delivery

*Corresponding author: Department of Bioengineering, University of California, San Diego, 9500 Gilman Drive, Mail Code 0412, La Jolla, CA 92093-0412, USA. Tel.: +1 858 822 7920; Fax: +1 858 534 5722. svarghese@ucsd.edu (S. Varghese).

Conflict of interest

Authors declare no conflict of interest.

Author Contributions

M.K., Y.-R.V.S., and S.V. designed the experiments. M.K., Y.-R.V.S., D.O.V. performed the experiments. M.K., Y.-R.V.S., and S.V. analyzed the data. M.K., Y.-R.V.S., and S.V. wrote the paper.

1. Introduction

Harnessing the ability of stem cells to promote regeneration of compromised tissues could be of great potential to wound healing, tissue repair, and reinstating the functionality of dysfunctional tissues/organs. There is a surge of interest in cell-based therapies to treat various debilitating diseases [1–6]. According to the clinical trial database, as of December 2014, over 4,000 registered clinical trials involving stem cells are underway [7]. Stem cell transplantation can contribute to tissue regeneration and repair either by differentiating into tissue specific cells or by the secretion of trophic factors to rejuvenate the host tissue environment [8–11]. Despite the enormous potential, cell transplantation procedures are still in its infancy, in part due to poor to moderate donor cell retention and survival following transplantation [6]. The hostile environment presented by the local tissue has been considered an important contributor towards the poor outcome of cell-transplantation therapies.

Different approaches, such as cell surface modifications and biomaterial-supported deliveries, have been explored to improve the likely outcome of cell transplantation [1, 12–16]. One such biomaterial-assisted cell delivery approach utilizes degradable hydrogels [17, 18]. Hydrogels are ideal candidates for cell delivery owing to their many soft tissue-like properties [19–21]. Hydrogels containing photolabile groups have been used to deliver cells in a controlled manner [22]. However, the materials undergoing photodegradation largely rely on UV light [22, 23]. Studies have also utilized hydrogels containing MMP-sensitive groups to achieve delivery of cells [13]. MMP-sensitive hydrogels are attractive as they rely on cell secreted MMPs to degrade the matrix [24–27]. However, they may not be ideal when fast degradation (~ hours) of the cell carriers is needed to deliver the cargo [13]. Furthermore, MMP-mediated degradation of hydrogels is dependent upon the level of MMPs and could vary significantly from tissue to tissue and their health states [28].

In this study, we investigated whether the incorporation of disulfide moieties onto the backbone of hydrogels could impart them with degradation properties that can be controlled by the encapsulated cells themselves to assist their delivery. Disulfide functional groups, two covalently bonded sulfur atoms, with a bond energy of ~ 60 kcal mol^{-1} are labile to thiol groups and reducing agents, such as glutathione, a cell metabolite [29, 30]. Thiol-disulfide shuffling is a key reaction in living systems [31, 32] with disulfide bonds playing an important role in protein folding and function [32–35]. Given their importance in biological systems and their unique functions, macromolecules containing disulfide moieties have been extensively studied for their chemistry [30, 36], kinetics [37], and thermodynamics [38]. Biomaterials containing disulfide groups have also been studied for drug [39, 40] and gene delivery [41, 42] as well as scaffolds for tissue engineering [43, 44]. In this study, we have synthesized disulfide modified PEG diacrylates to form cell-responsive hydrogels. Our results show that the PEG hydrogels containing disulfide moieties on their backbone form stable hydrogels and support stem cell encapsulation. The hydrogels were found to degrade in response to cell-secreted molecules *in vitro* and *in vivo*. The degradation kinetic of the hydrogels can be tuned by varying the fraction of disulfide moieties.

2. Materials and methods

2.1. Materials

Poly(ethylene glycol) (PEG; M_n 2000 Da and 3350 Da), acryloyl chloride, cystamine dihydrochloride, L-cysteine (Cys), reduced glutathione (GSH), calcium hydride, dexamethasone, β-glycerophosphate, ascorbic acid, indomethacin, isobutyl methylxanthine, insulin, pyridine, activated charcoal, and Sephadex G-25 were purchased from Sigma-Aldrich (USA). The disuccinimidyl carbonate was obtained from Acros Organics (USA). Dulbecco's modified eagle medium (DMEM; high glucose) was purchased from Hyclone. Fetal bovine serum (FBS), penicillin, and streptomycin were purchased from Gibco. Anhydrous Dichloromethane (DCM), acetonitrile, anhydrous diethyl ether, dithiothreitol (DTT), tris (2-carboxyethyl) phosphine (TCEP), potassium bicarbonate (K_2CO_3), potassium iodide (KI), hydrochloric acid (HCl), anhydrous sodium sulphate, sodium chloride (NaCl) and Celite 545 were purchased from Fisher Scientific. DCM and acetonitrile were dried using calcium hydride. Irgacure (D2959) was procured from Ciba, Switzerland. CellTracker Red (CMTPX) and Live/Dead assay kit were obtained from Life Technologies.

2.2 Synthesis of macromolecules

We have synthesized disulfide-modified poly(ethyle glycol) diacrylate (dPEGDA) (Fig. 1A), poly(ethylene glycol) diaminoethanol diacrylate (PEGDEDA) (Fig. 1B), and poly(ethylene glycol) diacrylate (PEGDA) (Fig. 1C). These macromolecules were utilized to create chemically crosslinked hydrogels.

(a) Synthesis of disulfide-modified poly(ethylene glycol) diacrylate (dPEGDA)—The synthesis of dPEGDA involves multiple reaction steps (Fig. 1A). The product dPEGDA (O) and the intermediate products, monoacrylate poly(ethylene glycol) (M) and monoacrylate-PEG-disuccinimidyl carbonate (N) are shown in the scheme. The details of each reaction step are provided below.

(a.1) Synthesis of monoacrylate poly(ethylene glycol) (M): Monoacrylate poly(ethylene glycol) (monoacrylate PEG) was prepared by adapting a previously reported method [45]. Briefly, 10 g of PEG (M_n 2000 Da), 1.737 g (7.5 mmol, 1.5 eq) of Ag_2O, 0.445 mL (0.497 g, 5.5 mmol, 1.1 eq) of acryloyl chloride, and 0.249 g (1.5 mmol, 0.3 eq) of KI were added into 100 mL of anhydrous DCM and stirred overnight at 4°C. The resulting solution was filtered, dried using a rotovap, and dissolved in deionized (DI) H_2O. The pH was adjusted to pH 3 by using 4 N HCl and stirred for 1 hour at 37°C. Activated charcoal was added to the mixture and stirred for 20 minutes. The solution was subsequently filtered and excess sodium chloride was added into the filtrate. The product was extracted using DCM followed by washing with 2 M K_2CO_3 and dried over anhydrous sodium sulfate. The product was precipitated in diethyl ether, dried under vacuum at room temperature, and stored at −20°C. The presence of peaks between 5.93 to 6.14 ppm in the ^{1}H-NMR spectra of the monoacrylated poly(ethylene glycol) (Fig. 2A) confirms the grafting of acrylate moiety onto the PEG molecule. The integration of the methylene protons at 3.63 ppm and the acrylate protons between 5.93 to 6.14 ppm suggests around 96% grafting efficiency.

^{1}H-NMR (300 MHz, $CDCl_3$, δ): 6.41–6.38 ppm (d, 1H), 6.19–6.13 ppm (dd, 1H), 5.95–5.93 (d, 1H), 4.3–4.28 ppm (t, 2H) and 3.77–3.5 ppm (broad) (Fig. 2A).

(a.2) Synthesis of monoacrylate-PEG-succinimidyl carbonate (N): One gram of monoacrylate poly(ethylene glycol) (M) was added to 0.512 g (2 mmol, 4 eq) of disuccinimidyl carbonate and 44 μL (0.55 mmol, 1.1 eq) of pyridine in 10 mL anhydrous acetonitrile under argon and stirred overnight at room temperature (Fig. 1A). The reaction mixture was dried using a rotovap and re-dissolved in anhydrous DCM. Monoacrylate-PEG-succinimidyl carbonate was isolated via phase separation in acetate buffer (0.1 M, pH 4.5, 15% sodium chloride) followed by washing with ice cold brine and finally dried over anhydrous sodium sulphate, filtered, and precipitated in diethyl ether. The product, monoacryloylate-PEG-succinimidyl carbonate, was filtered, washed with diethyl ether, dried under vacuum, and directly used for the next step reaction.

(a.3) Synthesis of disulfide-modified poly(ethylene glycol) diacrylate (dPEGDA) (O): One equivalent of monoacrylate-PEG-succinimydyl carbonate (N) was added into 0.3 equivalent of cystamine dihydrochloride (10 mg/mL) solution in 50 mM carbonate buffer (pH 8.5) (Fig. 1A). The reaction mixture was stirred for 4 hours at room temperature. The reaction mixture was purified using a Sephadex G–z25 column and lyophilized. The lyophilized product, dPEGDA, was stored at −20°C. The successful synthesis of dPEGDA was confirmed by FT-IR (Fig. S1) and ^{1}H-NMR (Fig. 2B).

^{1}H-NMR (300 MHz, $CDCl_3$, δ): 6.40–6.37 ppm (d, 1H), 6.18–6.12 ppm (dd, 1H), 5.94–5.92 ppm (d, 1H), 4.28–4.27 ppm (d, 4H), 4.14–4.13 ppm (d, 4H), 3.76–3.47 ppm (broad), 3.39 ppm (s, 4H) and 2.78 ppm (s, 4H) (Fig. 2B).

(b) Synthesis of poly(ethylene glycol) diaminoethanol diacrylate (PEGDEDA)—The product poly(ethylene glycol) diaminoethanol diacrylate (R) and the intermediate products, PEG-di-*p*-nitrophenyl carbonate (P) and diamino ethanol-modified poly(ethylene glycol) (Q), are shown in Fig. 1B. The details of each reaction step are provided below.

(b.1) Synthesis of PEG-di-p-nitrophenyl carbonate (P): Polyethyene glycol (PEG, M_n 3350 Da) was modified with *p*-nitrophenyl carbonate as previously reported [46]. Briefly, 5 g (1.49 mmol) of PEG and 0.630 mL (4.47 mmol, 3 eq) of triethylamine was added into 25 mL anhydrous acetonitrile. The reaction mixture was stirred for 15 minutes followed by addition of 0.884 g (4.47 mmol, 3 eq) of *p*-nitrophenyl chloroformate. After stirring for 24 hours at room temperature, the precipitated triethylammonium chloride was filtered, excess ethyl ether was added and the solution was left to crystallize at 4°C. The product was filtered, washed with diethyl ether, and recrystallized using acetonitrile-ether.

^{1}H-NMR (300 MHz, $CDCl_3$, δ): 8.29–8.27 ppm (d, 4H), 7.42–7.40 ppm (d, 4H), 4.41 ppm (s, 4H) and 3.79–3.47 ppm (broad) (Fig. S2A).

(b.2) Synthesis of diaminoethanol-modified poly(ethylene glycol) (Q): Two grams of PEG di-*p*-nitrophenyl carbonate (P) was added to 10 mL of 0.1 M borate buffer (pH 9.3) containing 0.21 mL of aminoethanol (12.69 mmol, 6 eq). The reaction mixture was

vigorously stirred for 4 hours at room temperature. The product was purified using a Sephadex G–25 column and lyophilized.

^{1}H-NMR (300 MHz, CDCl3, δ): 4.14 ppm (d, 4H), 3.77–3.48 ppm (broad), and 3.19 ppm (t, 4H) (Fig. S2B).

(b.3) Synthesis of poly(ethylene glycol) diaminoethanol diacrylate (PEGDEDA) (R): Two grams of dried diaminoethanol-modified PEG (Q) was dissolved in 20 mL of anhydrous DCM followed by addition of 0.239 mL (1.71 mmol, 3 eq) of triethylamine. The reaction mixture was stirred for 15 minutes followed by dropwise addition of 0.138 mL (1.71 mmol, 3 eq) of acryloyl chloride with vigorous stirring. The reaction mixture was stirred for additional 24 hours at room temperature. Upon completion of the reaction, excess diethyl ether was added and kept at 4°C for a few hours to precipitate the product. The product, PEGDEDA, was filtered and recrystallized thrice from DCM–ethyl ether mixture. The product was further purified using a Sephadex G-25 column and lyophilized.

^{1}H-NMR (300 MHz, $CDCl_3$): 6.44–6.38 ppm (d, 2H), 6.19–6.14 ppm (dd, 2H), 5.97–5.95 ppm (d, 2H), 4.22–4.17 (dd, 8H), 3.79–3.52 ppm (broad), and 3.42 ppm (d, 4H) (Fig. S2C).

(c) Synthesis of poly(ethylene glycol) diacrylate (PEGDA) (S)—Poly(ethylene glycol)-diacrylate (PEGDA) was prepared as previously described (Fig. 1C) [47]. Briefly, 10 g of PEG (M_n 3350 Da, 2.98 mmol) was dissolved in 250 mL of toluene at 127°C, followed by refluxing for 4 hours with vigorous stirring. Azeotropic distillation was used to remove the traces of water from the reaction mixture. On cooling this solution to room temperature (~25°C), 1 mL (7.46 mmol, 2.5 eq) of triethylamine was added with vigorous stirring. The reaction mixture was transferred to an ice bath at 4°C. To this reaction mixture, 0.6 mL (7.46 mmol, 2.5 eq) of acryloyl chloride in 15 mL of anhydrous DCM was added in dropwise manner for 30 minutes. The reaction mixture was raised to 45°C and stirred overnight. The reaction mixture was filtered through diatomaceous earth (Celite 545) to remove quaternary ammonium salt. The filtrate was concentrated using a rotovap and precipitated in excess diethyl ether. Precipitated product was redissolved in DCM and reprecipitated in diethyl ether. The resultant PEGDA was filtered and dried under vacuum at room temperature for 24 hours. The PEGDA was further purified using a Sephadex G-25 column and lyophilized.

^{1}H-NMR (300 MHz, $CDCl_3$, δ): 6.39–6.36 ppm (d, 2H), 6.17–6.11 ppm (dd, 2H), 5.93–5.91 ppm (d, 2H), 4.28–4.26 (t, 4H), 3.75–3.74 ppm (m, 8H), 3.62 ppm (broad), and 3.48–3.47 ppm (t, 4H). (Fig. S3)

2.3 ^{1}H-NMR and FT-IR

The successful syntheses of various products were confirmed through Fourier transform infrared (FT-IR) spectra and ^{1}H-Nuclear magnetic resonance (NMR). The Fourier transform infrared (FT-IR) spectra were recorded on Nicolet 6700 with Smart-iTR, equipped with liquid nitrogen-cooled MCT-A detector and diamond ATR crystal. ^{1}H-NMR experiments were carried out using Jeol ECA 500 MHz spectrometer.

2.4. Hydrogel preparation

The macromolecules were dissolved in DI water to yield final concentrations of 10, 15, or 20-wt% followed by mixing with Irgacure at a final concentration of 0.05% (wt/vol). Around 60 μL of the homogeneous solution was poured into a cylindrical mold (5 mm diameter) and exposed to UV irradiation (365 nm light at 4.5 mW/cm^2) for 5 minutes. The hydrogels were removed from the mold and washed thoroughly with DI water for 24 hours to eliminate unreacted reactants. The equilibrium-swollen hydrogels were dried at 60°C under vacuum until a constant weight was achieved. Dried hydrogels were used to study the swelling ratio in PBS and degradation kinetics in the presence of various degrading agents.

2.5. Swelling ratio measurements

The swelling ratios of the dPEGDA hydrogels were measured using a gravimetric method [48]. Each sample was immersed in PBS at 37°C and the swollen weights of the hydrogels were measured every hour after removal of excess water from the surface using a tissue paper. The swelling ratios of the samples were determined as a ratio of weights of swollen hydrogel (W_t) to dried hydrogel (W_0).

2.6. Small molecule-mediated degradation of dPEGDA hydrogels

Degradation of dPEGDA hydrogels containing different precursor concentrations (10 and 15-wt %) were examined in the presence of various disulfide reducing agents such as L-cysteine (Cys), reduced glutathione (GSH), dithiothreitol (DTT), and Tris (2-carboxyethyl)phosphine hydrochloride (TCEP). The dried hydrogels were incubated at 37°C in 2 mL of 10 mM phosphate buffered saline (PBS) containing various concentrations (0.5 and 1 mM) of the above listed molecules. The degradation of the hydrogels was evaluated by measuring swelling ratio variations as a function of time in the presence of different degrading agents. Hydrogels incubated in PBS were used as control. Degradation time was defined as the time taken by the hydrogels to be completely disintegrated.

2.7. pH-sensitive degradation

To determine the effect of pH on dPEGDA degradation, the hydrogels were incubated in buffers containing varying pHs; pH 5 (acetate buffer 50 mM), pH 7.4 (PBS 50 mM), and pH 9 (carbonate buffer 50 mM). Dried hydrogels were incubated at 37°C in 2 mL buffer solution. The degradation of hydrogels was evaluated by measuring swelling ratio variations as a function of time.

2.8. Cell culture

Human mesenchymal stem cells (hMSCs) (Institute for Regenerative Medicine, Texas A&M University) were cultured in growth medium (high glucose supplemented with 10% (vol/vol) FBS, 100 units/mL of penicillin, and 100 μg/mL of streptomycin). The hMSCs were trypsinized upon reaching 70% confluence and passage 5 cells were used for the experiments. Human induced pluripotent stem cells (hiPSCs) were expanded on mitomycin C-treated mouse embryonic fibroblast (MEF) feeder cells with Knockout DMEM (Life Technologies) containing 10% knockout serum replacement (Life Technologies), 1% NEAA nonessential amino acids (Life Technologies), 10% human plasmanate (Talecris

Biotherapeutics), 1% Gluta-MAX (Life Technologies), 55 mM 2-mercaptoethanol (Life Technologies), and 1% penicillin/streptomycin (Life Technologies). 30 ng/mL of bFGF (basic fibroblast growth factor, Life Technologies) was added daily into the growth medium and cells were passaged using Accutase (Millipore) at 80% confluency [49].

2.9. Cell encapsulation

hMSCs and hiPSCs were encapsulated in hydrogels with various polymer precursors, such as dPEGDA, PEGDA, and PEGDEDA. To create the cell-laden hydrogels, the required amount of precursor was dissolved in PBS. Irgacure was added to the precursor solutions and mixed thoroughly to achieve a final 0.05% (wt/vol) concentration. The cells were dispersed within 60 μL of the precursor solution and photopolymerized by exposing them to a wavelength of 365 nm light at 4.5 mW/cm^2. The cell-laden hydrogels with dimensions of 5 mm (d) × 3 mm (h) were transferred into dishes and cultured in their respective growth medium.

For dPEGDA-PEGDA copolymer hydrogels, the precursors were first individually dissolved in PBS at 10-wt%, then mixed at a ratio of 3:1, 1:1, and 1:3 (dPEGDA:PEGDA) prior to gelation.

2.10. Cell viability test

The viability of encapsulated cells was determined by the Live/Dead Viability/Cytotoxicty kit (Life Technologies), which contains calcein-AM and ethidium homodimer–1. A working dye solution was made by mixing 0.5 μL of calcein-AM dye with 2 μL of ethidium homodimer-1 dye in 1 mL DMEM. Cell-laden hydrogels were washed with PBS and cut into thin slices. The slices were incubated in the working solution for 30 min. Images were collected using a fluorescent microscope.

2.11. Cell-mediated degradation of dPEGDA hydrogels

Cell-laden hydrogels were incubated in growth medium at 37°C and 5% CO_2. The cell-laden hydrogels were collected at pre-determined time points and lyophilized to get the final weight (W_f). The percentage of degradation of the hydrogels was calculated following the formula $(W_i\text{-}W_f)/W_i \times 100$. To determine the initial weight (W_i), the cell-laden hydrogels were lyophilized immediately after encapsulation. The number of cells released from the hydrogels was determined by counting the cells using a hemocytometer. Acellular hydrogels were used as a control.

2.12. In vitro differentiation of hMSCs released from the dPEGDA hydrogels

To determine the effect of cell encapsulation and subsequent release on the function of cells, we have examined osteogenic and adipogenic differentiation of released hMSCs. The hMSCs released from the dPEGDA hydrogels were cultured in either osteogenic medium (high glucose DMEM supplemented with 10% FBS, 10 nM dexamethasone, 10 mM β-glycerophosphate, and 0.2 mM ascorbic acid) or adipogenic medium (high glucose DMEM supplemented with 10% FBS, 100 nM dexamethasone, 200 μM indomethacin, 0.5 mM isobutyl methylxanthine, and 10 μg/mL insulin) [50]. The cells were cultured for 14 days

with media change every other day. The differentiation pattern was compared against hMSCs not subjected to encapsulation.

2.13. Characterization of differentiated hMSCs

Alkaline phosphatase staining for osteogenic differentiation—The cells were fixed with 4% formaldehyde for 20 min., stained with nitro-blue tetrazolium and 5-bromo-4-chloro-3′-indolyphosphate BCIP/NBT (Sigma-Aldrich) for 15 min, rinsed with DI water and imaged immediately [50].

Oil red O staining for adipogenic differentiation—An Oil red O stock solution was prepared by dissolving 30 mg Oil red O (Fluka) with 10 ml isopropanol (99%). A working solution was prepared immediately before staining by mixing 3 parts of Oil red O stock solution with 2 parts of DI water, incubating for 10 min. Prior to use, the working solution was filtered using a filter paper. For staining, cells were fixed with 4% formaldehyde for 20 min., stained with Oil red O working solution for 10 min., rinsed with DI water, and imaged immediately under a microscope [50].

2.14. Preparation of mouse dorsal skinfold window chamber

NIH Guide for laboratory animals was followed for the care and handling of the laboratory animals. The experimental protocols were approved by the Institutional Animal Care and Use Committee (IACUC) of the University of California, San Diego. The dorsal window chamber was mounted onto a 2 month-old immune deficient NOD.CB17-Prkdc^{scid}/J (NOD/SCID) mice (body weight of 25–30 g, Jackson labs). The mice window chamber model is widely used for microvascular studies in the unanaesthetized state, and the complete surgical technique is described in detail elsewhere [51]. Briefly, the animal was prepared for chamber implantation with an intraperitoneal injection of ketamine (100 mg/kg) and xylazine (10 mg/kg). After hair removal, sutures were used to lift the dorsal skin away from the animal, and one frame of the chamber was positioned on the animal's back. A chamber consisted of two identical titanium frames with a 10-mm circular window was used. With the aid of backlighting and a stereomicroscope, one side of the skin fold was removed following the outline of the window until only a thin layer of retractor muscle and the intact subcutaneous skin of the opposing side remained. Inclusion criteria: Mice were suitable for the experiments if microscopic examination of the tissue in the chamber observed under 650X magnification did not reveal signs of edema or bleeding. The cell-laden hydrogels of roughly 2 mm (d) × 0.2 mm (h) with 6×10^3 hMSCs were transplanted between the exposed tissue and the observation window, and the chamber was sealed by placing the other titanium frame. For the window chamber experiment, hMSCs were labeled with CellTracker Red according to manufacturer protocol. Briefly, cells were washed with PBS and stained with 10 μM CellTracker incubated in serum-free DMEM for 30 minutes in an incubator with 5% CO_2 at 37°C.

2.15 Transplantation of hMSCs into skeletal muscle

Prior to transplantation, three-month-old NOD/SCID mice were administered with ketamine (100 mg/kg) and xylazine (10 mg/kg). A 5 mm incision was made to the muscle and an approximate size of 1 mm^3 10-wt% dPEGDA hydrogel containing a cell density of 1×10^5

hMSCs in 60 μL was implanted into each quadricep or tibialis anterior muscle and sutured to immobilize them in place. The same number of hMSCs suspended in 15 μL of growth medium was injected into the skeletal muscle and used as controls. After 5 days of transplantation, muscles were harvested and embedded in Optimal Cutting Temperature compound (OCT) and cryosectioned at 20 μm thickness with a cryostat (Leika CM 3050) across the longitudinal plane.

2.16 Immunofluorescence staining and image analyses

The excised muscles were characterized to evaluate the retention of donor cells in the host tissues. For immunofluorescence staining, samples were fixed in 4% PFA for 15 min at room temperature, blocked with a blocking buffer containing 0.3% Triton X-100 and 3% bovine serum albumin in PBS for 1 hr at room temperature. Samples were stained with primary antibodies for human lamin A/C (1:100; Vector Laboratories) and laminin (1:200; Abcam) overnight at 4°C. Sections were incubated with goat anti-mouse Alexa 488 (1:250; Life Technologies), goat anti-rabbit Alexa 546 (1:250; Life Technologies) secondary antibodies, and Hoechst 33342 (2 mg/mL; Life Technologies) for 1 hr at room temperature. Imaging was performed using a fluorescence microscope (Carl Zeiss; Axio Observer A1). The number of transplanted human lamin A/C-positive cells in the host tissue from each image was quantified using NIH ImageJ software. Three muscle samples were used and images of six serial sections were analyzed per muscle sample to quantify the number of donor cells in the host tissue.

2.17. Fluorescence intravital microscopy

Fluorescence and bright-field intravital microscopy were used to examine the release of cells from the implanted cell-laden hydrogels *in vivo*. The animals were restrained in a tube and the protruding window chamber was fixed to the microscopic stage for imaging. Measurements were carried out using a 40X (LUMPFL-WIR, numerical aperture 0.8, Olympus) water immersion objective. Animals were given 10 min to adjust to the tube environment before any measurement. Detailed mappings of the chamber vasculature were made such that the same baseline could be maintained throughout the experiment. Sites of observation were chosen based on cell implantation location and distinctive anatomic landmark to easily and quickly reestablish the same fields at each observation time point. Eight to ten sites were selected for each preparation.

2.18. Statistical analysis

GraphPad Prism 5 was used to perform statistical analyses. Two groups were compared using two-tailed Student’s t-test. p-values measuring less than 0.05 were considered to be statistically significant.

3. Results

3.1 Synthesis and characterization of macromolecules

We have synthesized a series of macromolecules for hydrogel fabrication and to examine the potential of incorporating disulfide moieties onto the backbone of hydrogel network to achieve cell-mediated hydrogel degradation. Disulfide-modified poly(ethylene glycol)

diacrylate (dPEGDA) was synthesized by following an earlier reported method with slight modification [45]. The intermediate and final products were characterized by ^{1}H-NMR and FT-IR.

For the synthesis of dPEGDA, we have conjugated mPEG onto the end primary amines of a cystamine molecule. The presence of methylene protons of cystamine at 2.78 and 3.39 ppm in dPEGDA, ^{1}H-NMR spectra, which is absent in monoacrylated PEG, suggests successful grafting of monoacrylated PEGs onto cystamine. The integrated intensity of the NMR signal corresponding to the methylene proton of PEG at 3.63 ppm is double in dPEGDA when compared with monoacrylated PEG, suggesting that both the end amines of cystamine were conjugated with mono-acrylated PEG molecules (Fig. 2). The grafting efficiency was calculated to be 96%. The peaks at 1652 cm^{-1} and 1530 cm^{-1} in the FT-IR spectrum of dPEGDA (Fig. S1) indicate the presence of an amide-ester bond (-NH-CO-O-), which is absent in mPEG. Similar to dPEGDA, successful synthesis of PEGDEDA and PEGDA was confirmed by ^{1}H-NMR spectroscopy (Fig. S2 and S3).

3.2 Degradation kinetics of dPEGDA hydrogels in presence of small molecules

The chemical structure of the dPEGDA hydrogel and the potential break down of the network responding to the degrading agents is schematically shown in Fig. 3A. Prior to degradation studies, we examined the swelling behavior of dPEGDA hydrogels in PBS. Swelling behavior as a function of time indicated that the hydrogels reached equilibrium swelling of dPEGDA hydrogels within a few hours in PBS (Fig. 3B). As expected the equilibrium swelling decreased with increasing precursor concentration (10–20% wt/vol). Varying precursor concentration is used as a way to alter the crosslink density of hydrogels, where increasing precursor concentration increases crosslink density [52–55].

The swelling ratio curve of dPEGDA hydrogels incubated in the presence of various degrading agents showed two distinct phases — an initial rising phase and then a descending phase (Fig. 3C and D). The initial increase in swelling is due to the imbibing of the solvent by the hydrogel, which is subsequently outweighed by the degradation of the hydrogel. The equilibrium swelling value finally approaches zero due to complete disintegration of the hydrogel network. Both the chemical nature and concentration of the degrading agents had a significant effect on the degradation kinetics of the hydrogels. The time taken for 10- and 15-wt% dPEGDA hydrogel to degrade decreased as the concentration of the degrading agent in the medium increased (Fig. 3C and D and Fig. S4A and B). Furthermore, as the concentration of the dPEGDA precursors increased (10–15-wt%), which in turn increased the crosslink density, the time taken for the hydrogels to degrade increased (Fig. S4C and D).

We also investigated the stability of dPEGDA hydrogels in varying pHs (pH 5, 7.4, and 9) by incubating the hydrogels in different buffers. At a basic environment of pH 9, 10-wt% dPEGDA hydrogels were degraded completely within 39 hours whereas no such degradation was observed at pH 7.4 or pH 5 during the same experimental time (Fig. 3E). A prolonged 30-day exposure of the hydrogel at pH 7.4 and 5 showed ~5% and 14% degradation, respectively (Fig. S5).

3.3 Cell-mediated degradation of dPEGDA hydrogels: In vitro analyses

To determine cell-mediated degradation, we used both human mesenchymal stem cells (hMSCs) and human induced pluripotent stem cells (hiPSCs). The cells were encapsulated within the dPEGDA hydrogel using UV photo-polymerization and cultured in corresponding growth medium. Acellular hydrogels in growth medium were used as a control. Live/dead fluorescent staining indicated majority of the encapsulated cells to be viable, with a uniform distribution of the cells in the hydrogels (Fig. S6). This is consistent with previous reports, which have shown that both PEG-based hydrogels and photo-polymerization are efficient strategies to encase cells within a three-dimensional structure with minimal toxicity [56].

As hypothesized, the dPEGDA hydrogels exhibited degradation in the presence of cells without the need of any external stimuli (Fig. 4). Cell-mediated hydrogel degradation is expressed as percent degradation. For a 10-wt% dPEGDA hydrogel of 5 mm (diameter) × 3 mm (height) containing ~2×10^5 hMSCs, the network was completely disintegrated by 48 hours (Fig. 4A and B). Since the dPEGDA hydrogel exhibits cell-responsive degradation, it is conceivable that the number of cells within the hydrogel will be a key parameter in regulating the degradation kinetics of dPEGDA hydrogels. To this end, cell-laden dPEGDA hydrogels with varying numbers of hMSCs (5×10^4, 1×10^5, 2×10^5, 4×10^5) were created. The time required to undergo complete hydrogel disintegration increased as the number of cells decreased from 4×10^5 to 5×10^4 (Fig. 4B and Fig. S7). While 10-wt% dPEGDA hydrogels containing 4×10^5 underwent complete disintegration within 24 hours, hydrogels containing only 5×10^4 cells took ~ 72 hours to disintegrate into solution. The release profile of the encapsulated cells from the dPEGDA hydrogels at various time points is given in Fig. 4C. The corresponding acellular hydrogels showed minimal degradation during the course of the studies (Fig 4B).

The cell-mediated degradation of dPEGDA hydrogel was further verified using hiPSC-encapsulation. Similar to hMSCs, dPEGDA hydrogels exhibited a cell-density dependent degradation in presence of hiPSCs (Fig. S8A and B). Amongst hMSCs and hiPSCs, the dPEGDA hydrogels showed faster degradation in presence of hiPSCs. The 10-wt% dPEGDA hydrogels containing 2×10^5 hiPSCs underwent complete disintegration within 24 hrs whereas 10-wt% hydrogels containing similar number of hMSCs took 48 hrs to disintegrate into solution (Fig. S8C). Unlike in PBS and Dulbecco's Modified Eagle Medium (DMEM), prolonged incubation of the acellular dPEGDA hydrogels in growth media for 7 days resulted in a degradation of 26% for 10-wt% dPEGDA hydrogels (Fig. S9).

We also determined cell-mediated degradation of PEGDEDA hydrogels. The PEGDEDA precursors were designed to contain amide-ester units (-NH-CO-O-) and ester units (-O-CO-) similar to dPEGDA hydrogels but no disulfide groups in the backbone. The cell-mediated degradation of the PEGDEDA hydrogel was examined by encapsulating 2×10^5 hMSCs within 10-wt% hydrogels. Unlike dPEGDA, the PEGDEDA hydrogel did not exhibit any degradation over a period of 7 days (Fig. S10).

3.5 Tuning of cell-mediated degradation kinetics

We investigated the effect of disulfide concentration (varied through dPEGDA precursor concentration) on cell-mediated degradation of dPEGDA hydrogels. Our results showed that 15-wt% dPEGDA hydrogels containing 2×10^5 hMSCs took around 120 hours (~5 days) to completely degrade compared to 48 hours (~2 days) for 10-wt% dPEGDA hydrogels (Fig. 4D). In addition to varying the precursor concentration of dPEGDA, we also used copolymerization as a strategy to tailor the degradation of dPEGDA hydrogels. The dPEGDA macromolecules were copolymerized with non-degradable poly(ethylene glycol) diacrylate (PEGDA; M_n 3400 Da) macromolecules at varying weight ratios (dPEGDA:PEGDA of 1:0, 3:1, 1:1, 1:3, and 0:1). Figure 4E shows the degradation profile of dPEGDA-PEGDA copolymer hydrogels containing varying amounts of degradable disulfide units. For a given number of encapsulated hMSCs (2×10^5) and hydrogel precursor concentration, increasing the ratio of PEGDA to dPEGDA increases the degradation time. Results showed that 10-wt% hydrogels of 100% dPEGDA underwent complete degradation in 2 days whereas dPEGDA:PEGDA hydrogels with 3:1 and 1:1 ratio took 6 and 80 days, respectively, to undergo complete degradation. The dPEGDA:PEGDA hydrogels of 1:3 ratio exhibited only ~20% degradation by 90 days. No degradation of PEGDA hydrogels (10-wt %) was observed during the experimental time of 90 days (Fig. 4E).

3.6 In vitro differentiation of encapsulated cells

The differentiation function of cells that were encapsulated and released from the dPEGDA hydrogels was investigated. Specifically, we examined the osteogenic and adipogenic differentiation of hMSCs released from 10-wt% dPEGDA hydrogels and compared to that of unencapsulated cells (Fig. 5). Similar to unencapsulated cells (Fig. 5A and B), the released cells from hydrogels cultured in osteogenic medium for 14 days underwent osteogenic differentiation as evident from positive alkaline phosphatase staining (Fig. 5C). Furthermore, released cells from hydrogels exposed to adipogenic medium showed positive oil red O staining, a marker for adipocytes (Fig. 5D). No significant differences in the differentiation pattern were observed between encapsulated and unencapsulated cells.

3.7 hMSCs implanted with dPEGDA hydrogel: An in vivo analysis

Although cell-mediated degradation can be verified and studied in a defined manner by *in vitro* assays, discrete *in vivo* characterization is more challenging. In order to understand the cell-release profiles of cell-laden dPEGDA hydrogel within an *in vivo* host environment, we utilized a dorsal window chamber implanted in immune incompetent NOD/SCID mouse. The use of such a minimally invasive, *in vivo* platform would allow real time monitoring of cell release form the implant. The dPEGDA hydrogels (10-wt%) containing hMSCs were implanted within the window chamber and their degradation was monitored as a function of time. Prior to cell encapsulation, the hMSCs were labeled with CellTracker Red dye to observe the release of encapsulated cells from the hydrogels to the surrounding host tissue. The window chamber was implanted on the back of an animal (Fig. 6A). The hydrogel was visually apparent in the dorsal window chamber immediately after implantation (white arrow, Fig. 6B) but was not evident after 4 days when the hydrogel was completely degraded (Fig. 6C). Figure 6D shows the bright-field microscopic image of the implanted

hydrogel along with the host vasculature. Figures 6E–G show the images of the cell-laden dPEGDA implant as a function of time. Similar to *in vitro* findings, the encapsulated cells were released into the surrounding host tissue and were evident at 48 (Fig. 6F) and 72 hours (Fig. 6G) post-implantation. Furthermore, the cells released from the hydrogels were found to attach and reach to the surrounding host tissue (Fig. 6H).

To further determine the effect of dPEGDA hydrogel-mediated implantation of cells on their *in vivo* survival upon transplantation, we transplanted hMSC-laden dPEGDA hydrogels into skeletal muscle. The hydrogel-assisted survival of donor cells 5 days post-transplantation was compared against the same cell population injected in suspension without the aid of any biomaterials. The muscle sections were stained for human-specific lamin A/C, laminin, and nuclei (Fig. 6I). Our analyses showed hMSCs that were transplanted with dPEGDA hydrogels were more abundant in the host tissue compared to cells that were administered without the use of hydrogel. Quantification of lamin A/C positive cells, which indicates the presence of transplanted hMSCs, showed a significantly higher number of cells within the host tissue when implanted using dPEGDA hydrogels compared to the control group (Fig. 6J).

4. Discussion

This work describes the development of a synthetic hydrogel that can undergo degradation by responding to cell-secreted molecules. The cell-mediated degradation described in this study is different from that of matrix metalloproteinase (MMP)-sensitive hydrogels. To impart cell-mediated degradation, we have incorporated di-sulfide moieties, known to respond to various cell-secreted molecules such as glutathione, onto the backbone of PEG hydrogel, which we termed as dPEGDA. We used PEG hydrogel as a model system because PEG is a widely used biomaterial for cell encapsulation [55, 57]. Although the results described in this study focuses on PEG system, incorporation of di-sulfide moieties onto the polymer backbone can be adapted to render other biomaterials also cell responsive.

Our results show that the *in vitro* degradation rate of the dPEGDA hydrogels can be varied from hours to months and is found to be dependent upon the type of encapsulated cells, cell number, and fraction of disulfide moieties present in the hydrogel backbone. The faster degradation rate observed in this study is contrary to most of the previous studies reporting slower degradation kinetics for biomaterials containing disulfide units [58]. The faster degradation observed in our study could be attributed to the chemical environment of the polymer chain surrounding the disulfide moieties. Previous studies have shown that the chemical environment of the disulfide units play a key role in determining their degradation kinetics [59]. The presence of electronegative functional groups adjacent to the disulfide bonds in dPEGDA could make them more susceptible to cleavage and hence rendering the molecules with faster degradation kinetics.

The modified PEG containing disulfide moieties supported cell encapsulation and viability of the encapsulated cells. As hypothesized, the cell-laden dPEGDA hydrogels underwent degradation responding to cell-secreted molecules and released cells. This is consistent with our knowledge that the disulfide bonds can be cleaved by agents like reduced glutathione

and molecules containing thiol groups. Glutathione is a biosynthetic product of cells. In addition to the cell-secreted molecules, many cell surface molecules containing thiol groups could also aid the cleavage of the disulfide bonds. Our *in vitro* characterization suggests that the cell-mediated degradation of dPEGDA hydrogels is dependent upon the cell number and type of cells. This could be attributed to the differences in the amount of cell-secreted molecules or the presence of thiol groups. Our results show that the dPEGDA hydrogels, in the absence of any cells, are stable at physiological pH with minimal to no degradation during the experimental time. However, significantly higher degradation was observed at lower (pH 5) and higher pH (pH 9). The higher degradation at basic pH (pH 9) could be due to the hydroxyl groups reacting with the disulfide moieties leading to the generation of thiolate anions, resulting in the cleavage of disulfide bonds. On the other hand, the higher degradation at acidic pH 5 compared to pH 7.4 could be due to the presence of acid-sensitive amide-ester bonds (-NH-CO-O-) in the hydrogel backbone [60]. The acellular dPEGDA hydrogels that exhibited minimal to no degradation in PBS and DMEM showed a small extent of degradation in cell culture medium. This relatively higher degradation of acellular hydrogels in culture medium compared to DMEM could be attributed to the presence of fetal bovine serum, which contains various proteins and amino acids with thiol groups.

In addition to disulfide units, dPEGDA hydrogels also possess other functional groups like amide-ester units (-NH-CO-O-) and ester units (-O-CO-) that could contribute to their observed degradation. However, findings that the cell-mediated degradation was observed only with dPEGDA hydrogels and not with PEGDEDA hydrogels containing similar number of ester and amide-ester units, but no disulfide moieties suggest that the cell-mediated degradation was indeed due to the presence of disulfide units in the hydrogel network.

Similar to *in vitro* findings, the cell-laden dPEGDA hydrogels underwent degradation *in vivo* to release the cells to the host tissue environment. These hydrogels could potentially exhibit a faster degradation *in vivo* due to the presence of host cells and body fluid enriched with molecules capable of cleaving the disulfide units. However, the tunability of the dPEGDA hydrogel degradation through the fraction of disulfide moieties in the backbone can be used to design the cell delivery vehicle with the desired degradation profile. Hydrogel-assisted implantation of cells results in more cell survival within the transplanted tissue [61–64]. Consistent with previous studies, transplantation of the cells with dPEGDA hydrogels showed significantly higher donor cell retention within the host skeletal muscle tissue compared to injection of cells to the host tissue. This grants an advantage of a degradable delivery vehicle in which the degradation can be autonomously and partially controlled by the cell cargo once implanted *in vivo* and to retain cells in the desired location *in situ*.

5. Conclusion

In summary, this study describes the development of disulfide-containing PEG hydrogels with tunable degradation kinetics ranging from hours to months. The dPEGDA hydrogels are designed to undergo degradation responding to cell-secreted molecules, wherein the matrix degradation can be fine-tuned through cell density, crosslink density, and

copolymerization (or fraction of GSH-sensitive disulfide units). Such hydrogels whose degradation can be autonomously controlled by the cells to assist the release of the encapsulated cells to the host tissue could yield applications in cell transplantation and tissue engineering.

Supplementary Material

Refer to Web version on PubMed Central for supplementary material.

Acknowledgments

Authors gratefully acknowledge the financial support from National Institutes of Health (NIH, Grants 1 R01 AR063184-01A1, 5 R01-HL52684-13A1, and 1 R56-HL123015-01A1) and California Institute of Regenerative Medicine (CIRM, RN2-00945 and RT2-01889). The hMSCs used in this study were provided by Texas A&M University (NIH Grant P40RR017447). The authors thank Cynthia Walser and Priya Nayak for the surgical preparation of the animals.

References

1. Ballios BG, Cooke MJ, van der Kooy D, Shoichet MS. A hydrogel-based stem cell delivery system to treat retinal degenerative diseases. Biomaterials. 2010; 31:2555–64. [PubMed: 20056272]
2. Hwang Y, Suk S, Shih YR, Seo T, Du B, Xie Y, et al. WNT3A promotes myogenesis of human embryonic stem cells and enhances in vivo engraftment. Scientific reports. 2014; 4:5916. [PubMed: 25084050]
3. Passier R, van Laake LW, Mummery CL. Stem-cell-based therapy and lessons from the heart. Nature. 2008; 453:322–9. [PubMed: 18480813]
4. Schäffler A, Büchler C. Concise Review: Adipose Tissue-Derived Stromal Cells—Basic and Clinical Implications for Novel Cell-Based Therapies. STEM CELLS. 2007; 25:818–27. [PubMed: 17420225]
5. Segers VFM, Lee RT. Stem-cell therapy for cardiac disease. Nature. 2008; 451:937–42. [PubMed: 18288183]
6. Mooney DJ, Vandenburgh H. Cell delivery mechanisms for tissue repair. Cell stem cell. 2008; 2:205–13. [PubMed: 18371446]
7. ClinicalTrails.gov. Stem cells therapy. 2014.
8. Hwang NS, Zhang C, Hwang YS, Varghese S. Mesenchymal stem cell differentiation and roles in regenerative medicine. Wiley interdisciplinary reviews Systems biology and medicine. 2009; 1:97–106. [PubMed: 20835984]
9. Caplan AI, Dennis JE. Mesenchymal stem cells as trophic mediators. Journal of cellular biochemistry. 2006; 98:1076–84. [PubMed: 16619257]
10. Carr AJ, Smart MJ, Ramsden CM, Powner MB, da Cruz L, Coffey PJ. Development of human embryonic stem cell therapies for age-related macular degeneration. Trends in neurosciences. 2013; 36:385–95. [PubMed: 23601133]
11. Gonfiotti A, Jaus MO, Barale D, Baiguera S, Comin C, Lavorini F, et al. The first tissue-engineered airway transplantation: 5-year follow-up results. Lancet. 2014; 383:238–44. [PubMed: 24161821]
12. Vo TN, Kasper FK, Mikos AG. Strategies for controlled delivery of growth factors and cells for bone regeneration. Advanced drug delivery reviews. 2012; 64:1292–309. [PubMed: 22342771]
13. Fonseca KB, Gomes DB, Lee K, Santos SG, Sousa A, Silva EA, et al. Injectable MMP-Sensitive Alginate Hydrogels as hMSC Delivery Systems. Biomacromolecules. 2013; 15:380–90. [PubMed: 24345197]
14. Jeong JH, Schmidt JJ, Kohman RE, Zill AT, DeVolder RJ, Smith CE, et al. Leukocyte-Mimicking Stem Cell Delivery via in Situ Coating of Cells with a Bioactive Hyperbranched Polyglycerol. Journal of the American Chemical Society. 2013; 135:8770–3. [PubMed: 23590123]

15. Cezar CA, Kennedy SM, Mehta M, Weaver JC, Gu L, Vandenburgh H, et al. Biphasic Ferrogels for Triggered Drug and Cell Delivery. Advanced Healthcare Materials. 2014; 3:1869–76. [PubMed: 24862232]
16. Kabra H, Hwang Y, Lim HL, Kar M, Arya G, Varghese S. Biomimetic Material-Assisted Delivery of Human Embryonic Stem Cell Derivatives for Enhanced In Vivo Survival and Engraftment. ACS Biomaterials Science & Engineering. 2014; 1:7–12. [PubMed: 26280019]
17. Bensaïd W, Triffitt JT, Blanchat C, Oudina K, Sedel L, Petite H. A biodegradable fibrin scaffold for mesenchymal stem cell transplantation. Biomaterials. 2003; 24:2497–502. [PubMed: 12695076]
18. Liu SQ, Rachel Ee PL, Ke CY, Hedrick JL, Yang YY. Biodegradable poly(ethylene glycol)–peptide hydrogels with well-defined structure and properties for cell delivery. Biomaterials. 2009; 30:1453–61. [PubMed: 19097642]
19. Hwang N, Varghese S, Li H, Elisseeff J. Regulation of osteogenic and chondrogenic differentiation of mesenchymal stem cells in PEG-ECM hydrogels. Cell Tissue Res. 2011; 344:499–509. [PubMed: 21503601]
20. Varghese S, Elisseeff JH. Hydrogels for musculoskeletal tissue engineering. Adv Polym Sci. 2006:95–144.
21. Lutolf MP, Hubbell JA. Synthetic biomaterials as instructive extracellular microenvironments for morphogenesis in tissue engineering. Nat Biotechnol. 2005; 23:47–55. [PubMed: 15637621]
22. Griffin DR, Kasko AM. Photodegradable Macromers and Hydrogels for Live Cell Encapsulation and Release. Journal of the American Chemical Society. 2012; 134:13103–7. [PubMed: 22765384]
23. Kloxin AM, Kasko AM, Salinas CN, Anseth KS. Photodegradable Hydrogels for Dynamic Tuning of Physical and Chemical Properties. Science. 2009; 324:59–63. [PubMed: 19342581]
24. Patterson J, Hubbell JA. Enhanced proteolytic degradation of molecularly engineered PEG hydrogels in response to MMP-1 and MMP-2. Biomaterials. 2010; 31:7836–45. [PubMed: 20667588]
25. Lutolf MP, Lauer-Fields JL, Schmoekel HG, Metters AT, Weber FE, Fields GB, et al. Synthetic matrix metalloproteinase-sensitive hydrogels for the conduction of tissue regeneration: Engineering cell-invasion characteristics. Proceedings of the National Academy of Sciences. 2003; 100:5413–8.
26. Seliktar D, Zisch AH, Lutolf MP, Wrana JL, Hubbell JA. MMP-2 sensitive, VEGF-bearing bioactive hydrogels for promotion of vascular healing. Journal of Biomedical Materials Research Part A. 2004; 68A:704–16. [PubMed: 14986325]
27. Kim S, Chung EH, Gilbert M, Healy KE. Synthetic MMP-13 degradable ECMs based on poly(N-isopropylacrylamide-co-acrylic acid) semi-interpenetrating polymer networks. I. Degradation and cell migration. Journal of Biomedical Materials Research Part A. 2005; 75A:73–88. [PubMed: 16049978]
28. Komosinska-Vassev K, Olczyk P, Winsz-Szczotka K, Kuznik-Trocha K, Klimek K, Olczyk K. Age- and gender-dependent changes in connective tissue remodeling: physiological differences in circulating MMP-3, MMP-10, TIMP-1 and TIMP-2 level. Gerontology. 2011; 57:44–52. [PubMed: 20215736]
29. Houk J, Whitesides GM. STRUCTURE REACTIVITY RELATIONS FOR THIOL DISULFIDE INTERCHANGE. Journal of the American Chemical Society. 1987; 109:6825–36.
30. Lees WJ, Whitesides GM. Equilibrium constants for thiol-disulfide interchange reactions: a coherent, corrected set. The Journal of Organic Chemistry. 1993; 58:642–7.
31. Singh RW, GM. Thiol-disulfideinterchang. The chemistry of sulphur-containing functional groups. 1993:633–58.
32. Hansen RE, Roth D, Winther JR. Quantifying the global cellular thiol-disulfide status. Proceedings of the National Academy of Sciences of the United States of America. 2009; 106:422–7. [PubMed: 19122143]
33. Creighton TE. Disulphide bonds and protein stability. BioEssays. 1988; 8:57–63. [PubMed: 3282505]

34. Markovic I, Stantchev TS, Fields KH, Tiffany LJ, Tomic M, Weiss CD, et al. Thiol/disulfide exchange is a prerequisite for CXCR4-tropic HIV-1 envelope-mediated T-cell fusion during viral entry. Blood. 2004; 103:1586–94. [PubMed: 14592831]
35. Hogg PJ. Disulfide bonds as switches for protein function. Trends Biochem Sci. 2003; 28:210–4. [PubMed: 12713905]
36. Houk J, Whitesides GM. Structure-reactivity relations for thiol-disulfide interchange. Journal of the American Chemical Society. 1987; 109:6825–36.
37. Shaked, Ze; Szajewski, RP.; Whitesides, GM. Rates of thiol-disulfide interchange reactions involving proteins and kinetic measurements of thiol pKa values. Biochemistry. 1980; 19:4156–66. [PubMed: 6251863]
38. Jensen KS, Hansen RE, Winther JR. Kinetic and thermodynamic aspects of cellular thiol-disulfide redox regulation. Antioxidants & redox signaling. 2009; 11:1047–58. [PubMed: 19014315]
39. Koo AN, Lee HJ, Kim SE, Chang JH, Park C, Kim C, et al. Disulfide-cross-linked PEG-poly(amino acid)s copolymer micelles for glutathione-mediated intracellular drug delivery. Chemical Communications. 2008:6570–2. [PubMed: 19057782]
40. Saito G, Swanson JA, Lee K-D. Drug delivery strategy utilizing conjugation via reversible disulfide linkages: role and site of cellular reducing activities. Advanced drug delivery reviews. 2003; 55:199–215. [PubMed: 12564977]
41. Cai X, Dong C, Dong H, Wang G, Pauletti GM, Pan X, et al. Effective Gene Delivery Using Stimulus-Responsive Catiomer Designed with Redox-Sensitive Disulfide and Acid-Labile Imine Linkers. Biomacromolecules. 2012; 13:1024–34. [PubMed: 22443494]
42. Wang Y, Chen P, Shen J. The development and characterization of a glutathione-sensitive cross-linked polyethylenimine gene vector. Biomaterials. 2006; 27:5292–8. [PubMed: 16806454]
43. Yang F, Wang J, Hou J, Guo H, Liu C. Bone regeneration using cell-mediated responsive degradable PEG-based scaffolds incorporating with rhBMP-2. Biomaterials. 2013; 34:1514–28. [PubMed: 23187021]
44. Zhang J, Skardal A, Prestwich GD. Engineered extracellular matrices with cleavable crosslinkers for cell expansion and easy cell recovery. Biomaterials. 2008; 29:4521–31. [PubMed: 18768219]
45. Leslie-Barbick JE, Moon JJ, West JL. Covalently-Immobilized Vascular Endothelial Growth Factor Promotes Endothelial Cell Tubulogenesis in Poly(ethylene glycol) Diacrylate Hydrogels. Journal of Biomaterials Science, Polymer Edition. 2009; 20:1763–79. [PubMed: 19723440]
46. Veronese FM, Largajolli R, Boccu E, Benassi CA, Schiavon O. Surface modification of proteins. Activation of monomethoxy-polyethylene glycols by phenylchloroformates and modification of ribonuclease and superoxide dismutase. Applied biochemistry and biotechnology. 1985; 11:141–52. [PubMed: 4026282]
47. Lin S, Sangaj N, Razafiarison T, Zhang C, Varghese S. Influence of physical properties of biomaterials on cellular behavior. Pharmaceutical research. 2011; 28:1422–30. [PubMed: 21331474]
48. Zhang C, Aung A, Liao LQ, Varghese S. A novel single precursor-based biodegradable hydrogel with enhanced mechanical properties. Soft Matter. 2009; 5:3831–4.
49. Chang CW, Hwang Y, Brafman D, Hagan T, Phung C, Varghese S. Engineering cell-material interfaces for long-term expansion of human pluripotent stem cells. Biomaterials. 2013; 34:912–21. [PubMed: 23131532]
50. Varghese S, Hwang NS, Ferran A, Hillel A, Theprungsirikul P, Canver AC, et al. Engineering Musculoskeletal Tissues with Human Embryonic Germ Cell Derivatives. STEM CELLS. 2010; 28:765–74. [PubMed: 20178108]
51. Colantuoni, A.; Bertuglia, S.; Intaglietta, M. Quantitation of rhythmic diameter changes in arterial microcirculation. 1984.
52. Hoffman AS. Hydrogels for biomedical applications. Advanced drug delivery reviews. 2002; 54:3–12. [PubMed: 11755703]
53. Lin S, Sangaj N, Razafiarison T, Zhang C, Varghese S. Influence of Physical Properties of Biomaterials on Cellular Behavior. Pharm Res. 2011; 28:1422–30. [PubMed: 21331474]

54. Bryant S, Chowdhury T, Lee D, Bader D, Anseth K. Crosslinking Density Influences Chondrocyte Metabolism in Dynamically Loaded Photocrosslinked Poly(ethylene glycol) Hydrogels. Annals of Biomedical Engineering. 2004; 32:407–17. [PubMed: 15095815]

55. Nguyen QT, Hwang Y, Chen AC, Varghese S, Sah RL. Cartilage-like mechanical properties of poly (ethylene glycol)-diacrylate hydrogels. Biomaterials. 2012; 33:6682–90. [PubMed: 22749448]

56. Zhang C, Sangaj N, Hwang Y, Phadke A, Chang CW, Varghese S. Oligo(trimethylene carbonate)-poly(ethylene glycol)-oligo(trimethylene carbonate) triblock-based hydrogels for cartilage tissue engineering. Acta biomaterialia. 2011; 7:3362–9. [PubMed: 21664305]

57. Hwang NS, Varghese S, Elisseeff J. Derivation of chondrogenically-committed cells from human embryonic cells for cartilage tissue regeneration. PloS one. 2008; 3:e2498. [PubMed: 18575581]

58. Yang F, Wang J, Peng G, Fu SC, Zhang S, Liu CS. PEG-based bioresponsive hydrogels with redox-mediated formation and degradation. J Mater Sci-Mater M. 2012; 23:697–710. [PubMed: 22311074]

59. Parker AJ, Kharasch N. The Scission Of The Sulfur-Sulfur Bond. Chemical Reviews. 1959; 59:583–628.

60. Chen H, Li Y, Liu Y, Gong T, Wang L, Zhou S. Highly pH-sensitive polyurethane exhibiting shape memory and drug release. Polymer Chemistry. 2014; 5:5168–74.

61. Mayfield AE, Tilokee EL, Latham N, McNeill B, Lam BK, Ruel M, et al. The effect of encapsulation of cardiac stem cells within matrix-enriched hydrogel capsules on cell survival, post-ischemic cell retention and cardiac function. Biomaterials. 2014; 35:133–42. [PubMed: 24099706]

62. Sarnowska A, Jablonska A, Jurga M, Dainiak M, Strojek L, Drela K, et al. Encapsulation of Mesenchymal Stem Cells by Bioscaffolds Protects Cell Survival and Attenuates Neuroinflammatory Reaction in Injured Brain Tissue After Transplantation. Cell Transplant. 2013; 22:S67–S82. [PubMed: 24070175]

63. Liang Y, Walczak P, Bulte JWM. The survival of engrafted neural stem cells within hyaluronic acid hydrogels. Biomaterials. 2013; 34:5521–9. [PubMed: 23623429]

64. Karoubi G, Ormiston ML, Stewart DJ, Courtman DW. Single-cell hydrogel encapsulation for enhanced survival of human marrow stromal cells. Biomaterials. 2009; 30:5445–55. [PubMed: 19595454]

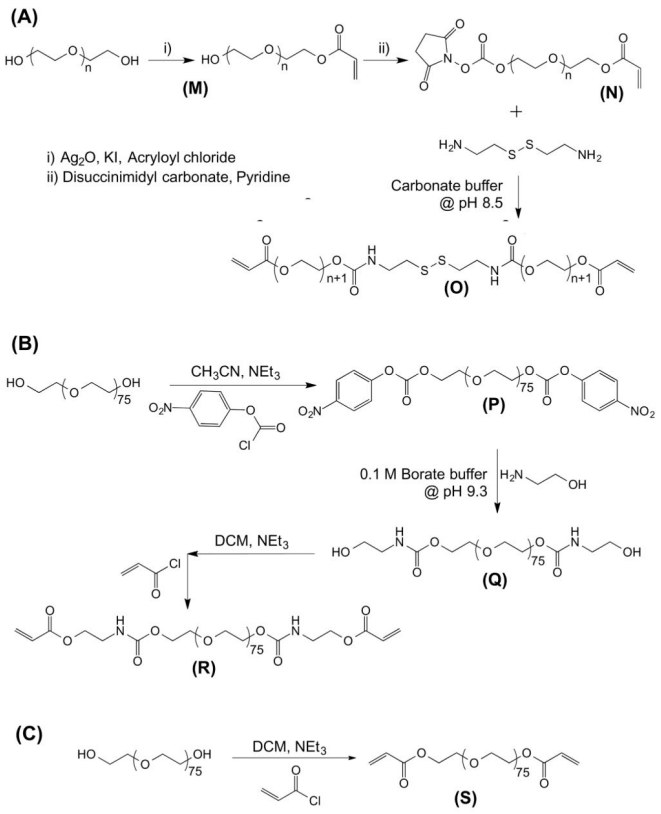

Figure 1.

Reaction scheme for the synthesis of (A) disulfide-modified poly(ethylene glycol) diacrylate (dPEGDA), (B) poly(ethylene glycol) diaminoethanol diacrylate (PEGDEDA), and (C) poly(ethylene glycol) diacrylate (PEGDA). Refer to Materials and methods section for individual molecules.

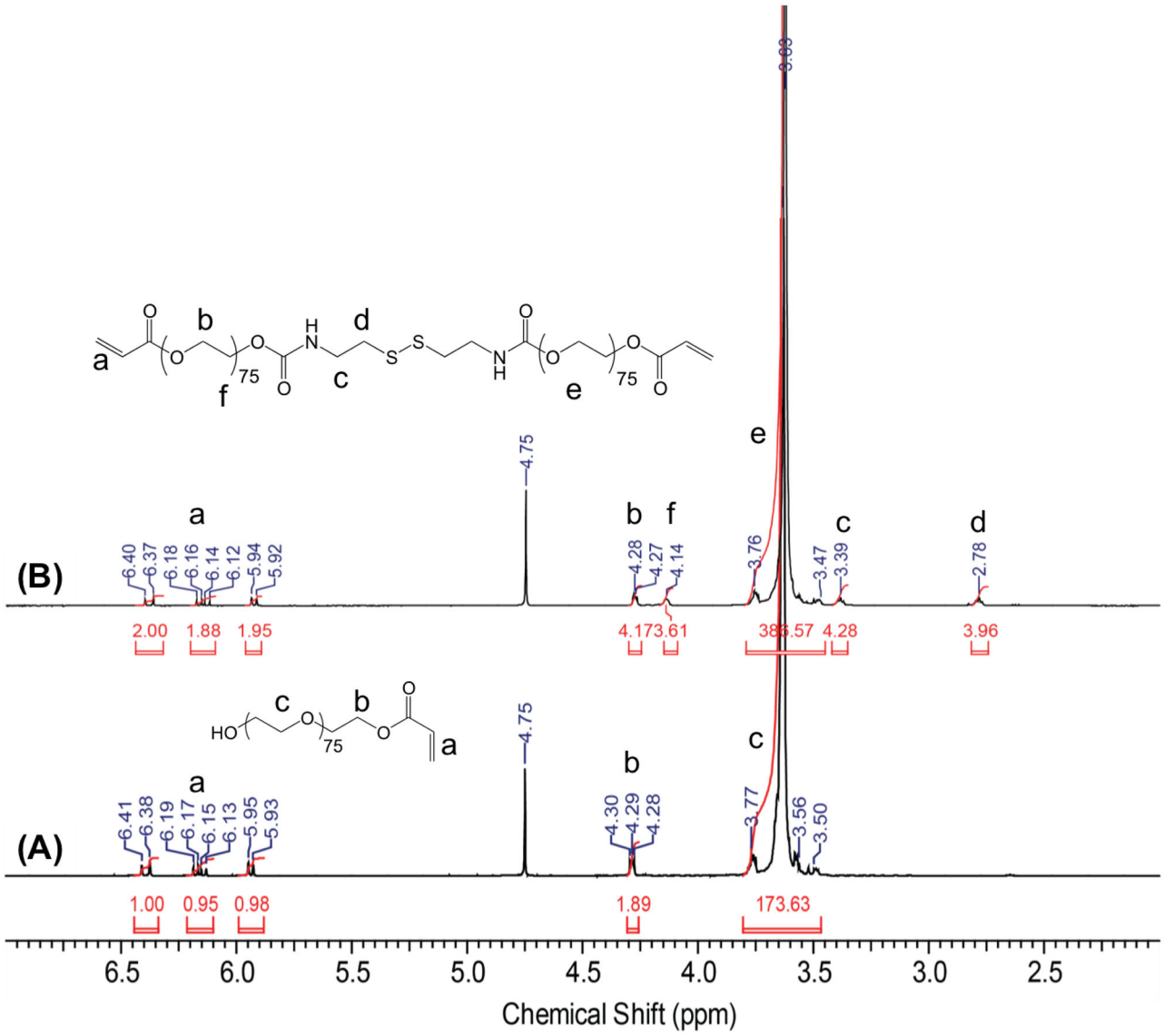

Figure 2.

^{1}H-NMR spectra of (A) monoacrylate PEG and (B) dPEGDA molecules.

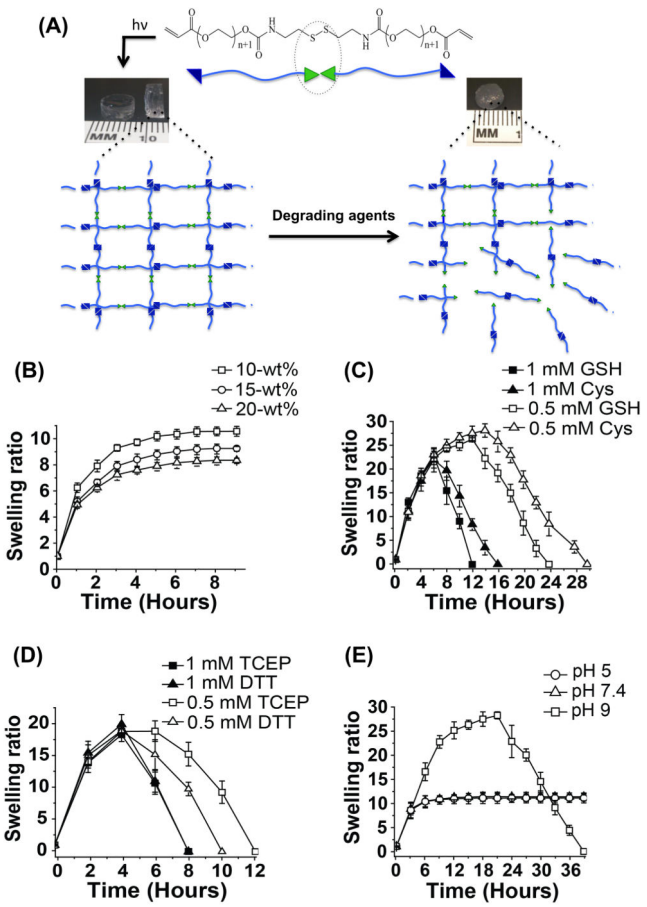

Figure 3.

Degradation of disulfide PEG diacrylate (dPEGDA) hydrogels. (A) Schematic representation of the molecular structure of disulfide PEG diacrylate (dPEGDA) oligomers and the hydrogel network before and after their degradation. The green triangles represent the disulfide units and the blue triangles represent the acrylate moieties. The degradation of the hydrogel scaffold occurs at the disulfide cleavage site (green) by either thiol-disulfide interchange or reduction of disulfide in the presence of various reducing agents. (B) Swelling ratio of dPEGDA hydrogels synthesized from precursor concentrations of 10–20-wt %. (C) Degradation of 10-wt% dPEGDA hydrogels in presence of 0.5 mM and 1 mM concentrations of cysteine (Cys) and reduced glutathione (GSH). (D) Degradation of 10-wt % dPEGDA hydrogels in 0.5 mM and 1 mM of dithiothreitol (DTT) and tris-(2-carboxyethyl)phosphine, hydrochloride (TCEP). (E) Degradation of 10-wt% dPEGDA hydrogels in pH 5, 7.4, and 9 buffers.

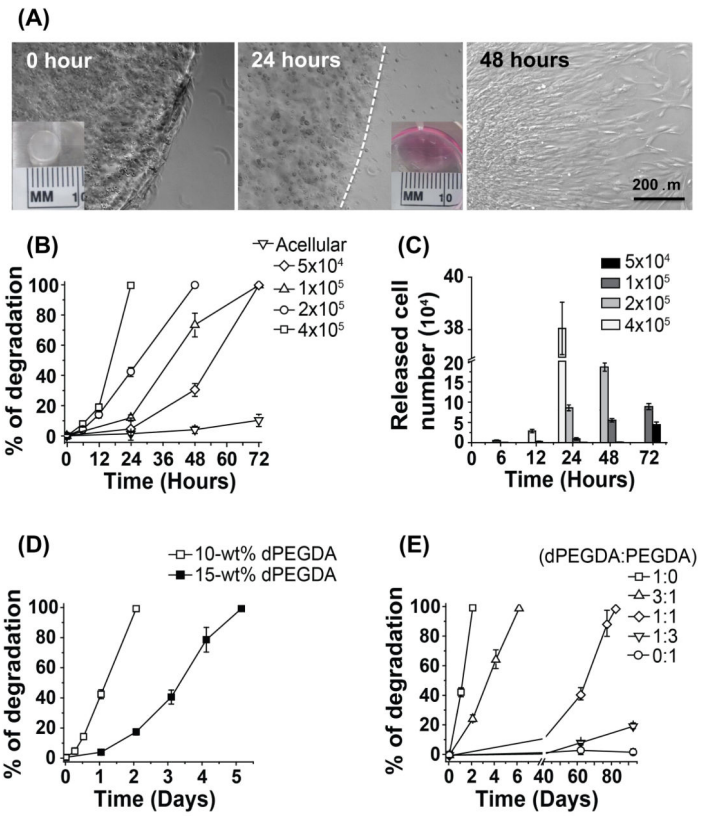

Figure 4.

Cell-mediated degradation of dPEGDA hydrogels. (A) Bright-field images of the release of hMSCs from a 10-wt% cell-laden dPEGDA hydrogel, containing 2×10^5 hMSCs, as a function of time (0 – 48 hours). The inset shows the gross image of the corresponding cell-laden hydrogel. Scale bar: 200 μm. (B) Degradation profile of 10-wt% dPEGDA hydrogels containing different numbers ($0 – 4 \times 10^5$) of hMSCs. (C) Number of hMSCs released from dPEGDA hydrogels containing varying numbers of encapsulated hMSCs. (D) Degradation profile of 10 and 15-wt% dPEGDA hydrogels encapsulating 2×10^5 hMSCs. (E) Degradation profile of 10-wt% copolymer hydrogels, encapsulated with 2×10^5 hMSCs, containing varying ratios of dPEGDA and PEGDA.

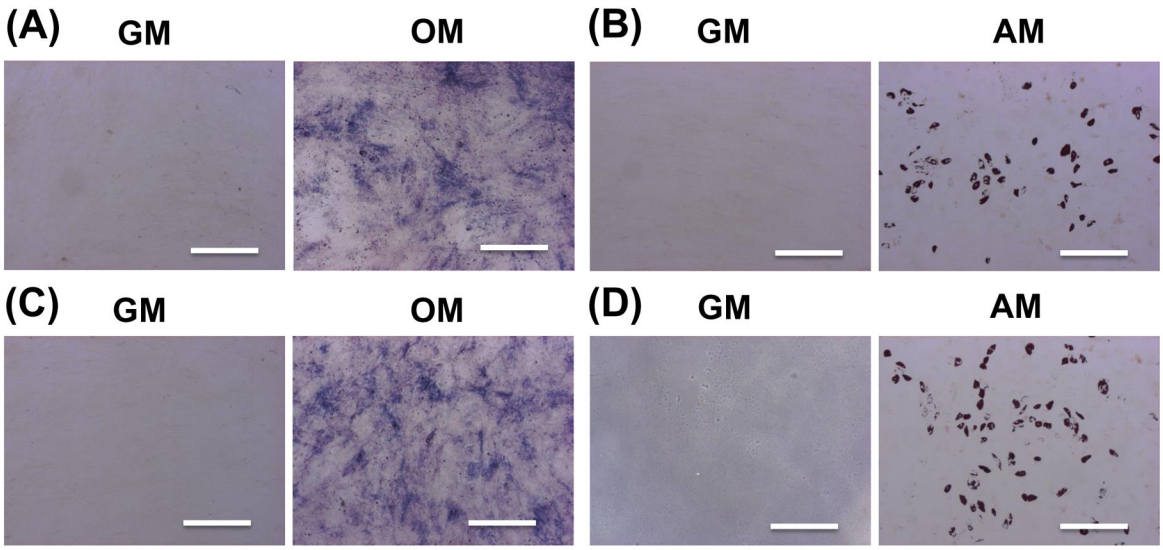

Figure 5.

Differentiation of hMSCs released from dPEGDA hydrogels. (A) Alkaline phosphatase staining and (B) oil red O staining of control (unencapsulated hMSCs) after 14 days of osteogenic and adipogenic differentiation, respectively. hMSCs that were encapsulated and released from hydrogels were stained for (C) alkaline phosphatase and (D) oil red O after 14 days of osteogenic and adipogenic differentiation, respectively. Scale bar: 200 μm. GM: growth medium. OM: osteogenic medium. AM: adipogenic medium.

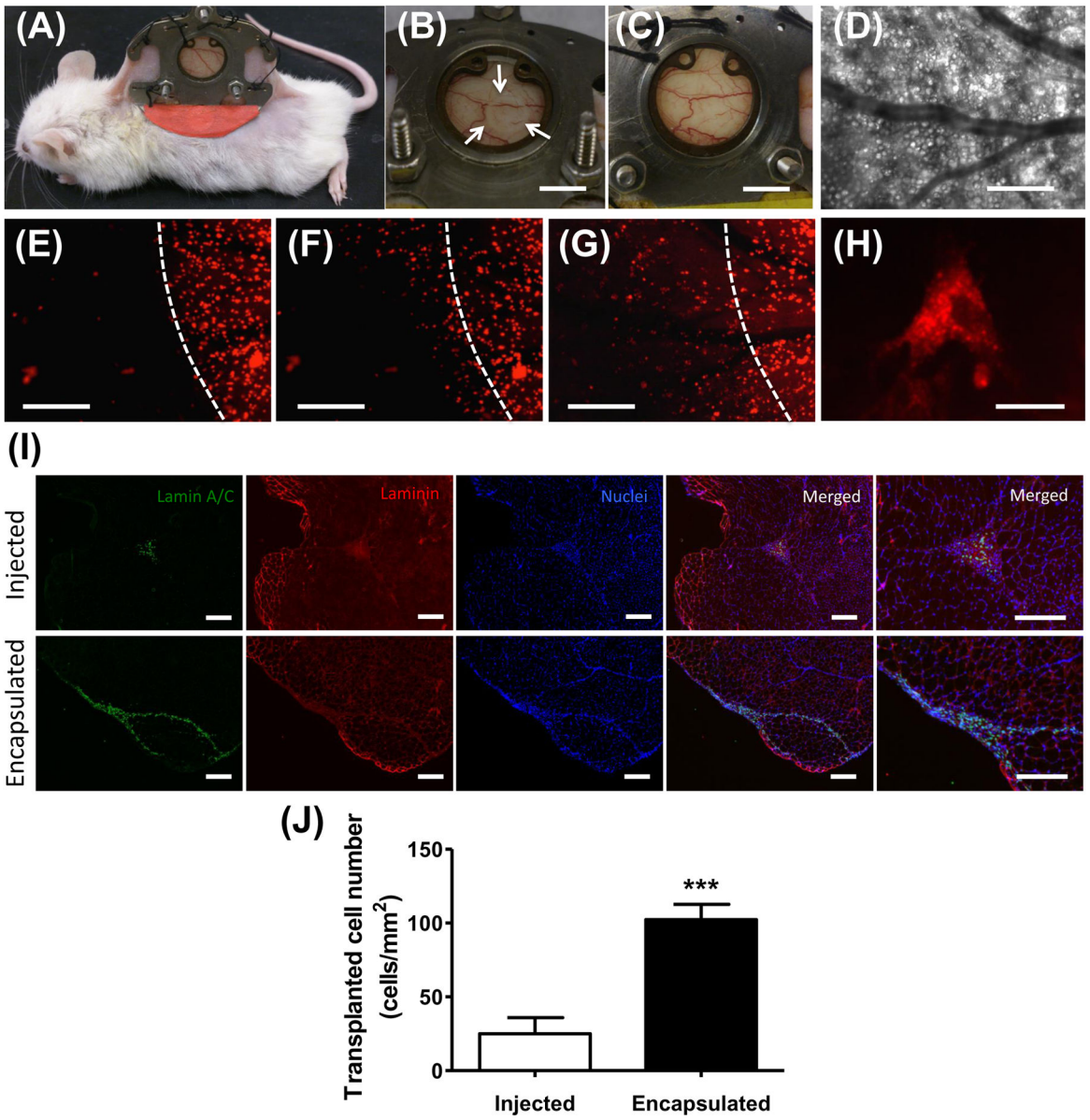

Figure 6.

In vivo analysis of cell release from cell-laden dPEGDA hydrogels. (A) Animal implanted with the dorsal window chamber. B) White arrows depict the circular hMSC-laden 10-wt% dPEGDA within the window chamber. (C) Same view of Fig. 5B depicting visual absence of hMSC-laden hydrogel after 4 days of implantation. Scale bar: 5 mm. (D–G) Intravital microscopic images of the same tissue site through the observation window. D) Brightfield image of subcutaneous tissue and vasculature. Imaging of the cell-laden hydrogel after (E) 24 hours, (F) 48 hours, and (G) 72 hours showing the release of the cells from the dPEGDA hydrogels. The cells are labeled with CellTracker Red. White line depicts the initial hydrogel boundary. Scale bar: 400 μm. (H) Released hMSCs that attached and spread on the subcutaneous tissue after 72 hours. Scale bar: 50 μm. (I) Immunofluorescent staining and (J) quantification of transplanted cells (human lamin A/C) in skeletal muscle of NOD/SCID

mice 5 days post implantation. Scale bar: 200 μm. Data are presented as the mean ± SEM (n = 3). Two groups were compared by two-tailed Student's t-test. Asterisks were assigned to p-values with statistical significance (***, $p < 0.001$).